

Organic Matter Complexation Promotes Fe(II) Oxidation by the Photoautotrophic Fe(II)-Oxidizer *Rhodopseudomonas palustris* TIE-1

Chao Peng,[†] Casey Bryce,[†] Anneli Sundman,[†] Thomas Borch,^{‡,§} and Andreas Kappler^{*,†}

[†]Geomicrobiology, Center for Applied Geoscience, University of Tuebingen, Sigwartstrasse 10, 72076 Tuebingen, Germany

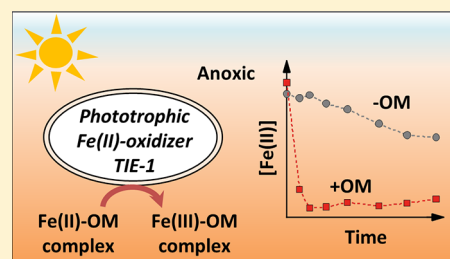
[‡]Department of Soil and Crop Sciences, Colorado State University, Fort Collins, Colorado 80523, United States

[§]Department of Chemistry, Colorado State University, Fort Collins, Colorado 80523, United States

Supporting Information

ABSTRACT: Fe(II)–organic matter (Fe(II)–OM) complexes are present in the photic zone of aquatic environments and due to their reactivity may play an important role in biogeochemical cycling. Complexation of Fe has been shown to influence the rates and extent of many chemical and microbial redox reactions. However, it is currently unknown whether, how fast, and to which extent Fe(II)–OM complexes can be oxidized by anoxygenic photoautotrophic Fe(II)-oxidizing microorganisms which are widespread in photic habitats and use electrons from Fe(II) to fix CO₂. Here, we used the photoautotrophic Fe(II)-oxidizer *Rhodopseudomonas palustris* TIE-1 to demonstrate that Fe(II) complexation by OM significantly accelerated the rates of Fe(II) oxidation by strain TIE-1 compared to the oxidation of nonorganically bound, free Fe(II), although a fraction of the Fe(II) present as Fe(II)–OM complexes seemed to resist microbial oxidation. Analysis of Fe–OM aggregate sizes showed that the remaining, nonoxidized Fe(II) and almost all of the Fe(III) in the Fe(II)–humic and Fe(II)–fulvic acid oxidation products were in the form of colloids (3–200 nm). In summary, this study shows that Fe(II)–OM complexes can be oxidized microbially in the photic zone, and the complexation of Fe(II) by OM controls the kinetics and extent of Fe(II) oxidation.

KEYWORDS: iron-organic-matter complexes, redox, iron geomicrobiology, electron transfer, photoferrotroph, anoxygenic photosynthesis



INTRODUCTION

The oxidation of Fe(II) at neutral pH forms poorly soluble Fe(III) which typically leads to precipitation of Fe(III) minerals with reactive surfaces and large binding capacities. This immobilization of Fe(III) in minerals influences iron bioavailability in the environment and can also influence the fate and turnover of other elements and compounds, from organic carbon¹ to toxic heavy metal(loid)s such as As and Cd^{2–4} and other environmental contaminants.⁵ At neutral pH, Fe(II) can be rapidly oxidized chemically by molecular oxygen to Fe(III). Alternatively, Fe(II)-oxidizing microorganisms can also catalyze this reaction coupled to reduction of O₂ or nitrate or photosynthetically during CO₂ fixation.⁶ Photoautotrophic Fe(II)-oxidizing microorganisms are widely distributed in freshwater and marine habitats, including photic zones of water columns and sediments.⁷ These bacteria gain energy from anoxygenic photosynthesis, oxidizing Fe(II), and utilizing the electrons for CO₂ fixation.^{6,8} The photoautotrophic Fe(II)-oxidizer *Rhodopseudomonas palustris* TIE-1⁹ is thought to be able to enzymatically oxidize Fe(II) via a c-type cytochrome¹⁰ at the surface of the cell membrane.¹¹ Strain TIE-1 has been shown to be capable of oxidizing Fe(II) in the mineral magnetite¹² and utilizing electrons directly from poised electrodes.¹³

In the natural environment, Fe(II) is not only found as free Fe(II) or in Fe(II)-containing minerals, it is often complexed with organic matter which has been shown to strongly influence the environmental behavior of Fe. Such Fe(II)–organic-matter (Fe(II)–OM) complexes are abundant in nature.^{14–21} For example, more than 99% of the Fe in the ocean is found to be complexed by OM.²² OM complexation influences the rates of abiotic oxidation of Fe(II) by O₂^{23–26} and nitrite.²⁷ Indeed, the complexation and stabilization of Fe(II) by organic ligands was suggested to be the main reason for higher than expected abundances of Fe(II) in many oxic aquatic environments.^{18,19,22,28} Recent work has also shown that Fe(II)–OM complexation strongly inhibits microbial nitrate-dependent Fe(II) oxidation.²⁹ However, it is currently unknown whether and how Fe(II)–OM complexation influences microbial photoautotrophic Fe(II) oxidation.

In this study, we aim to determine how Fe(II)–OM complexation influences the oxidation of Fe(II) by the photoautotrophic Fe(II)-oxidizing strain *R. palustris* TIE-1. The kinetics, extent of oxidation of Fe(II)–OM complexes,

Special Issue: Iron Redox Chemistry and Its Environmental Impact

Received: January 29, 2019

Accepted: February 25, 2019

Published: February 25, 2019

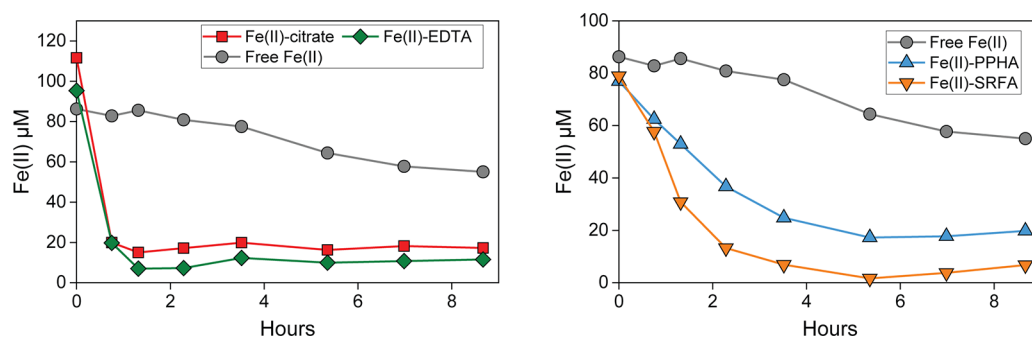


Figure 1. Oxidation of different Fe(II)–OM complexes by *R. palustris* TIE-1. Fe(II) was present in the form of either non-OM-bound, free Fe(II) (gray circles), Fe(II)–citrate (red squares), or Fe(II)–EDTA (green diamonds) (left panel) or as Fe(II)–PPHA complexes (blue triangles) or Fe(II)–SRFA complexes (yellow triangle) (right panel). The results are reported as an average of triplicate measurements. Because duplicate microbiological setups showed very similar results, representative results out of these duplicate setups are shown here, and the second one is shown in the Supporting Information Figure S2.

and the size fractions of Fe in their oxidation products are compared to non-OM-complexed free Fe(II).

MATERIALS AND METHODS

To determine how Fe(II)–OM complexation influences photoautotrophic Fe(II) oxidation, we performed separate cell suspension experiments with the photoautotrophic Fe(II)-oxidizer *R. palustris* TIE-1 with either Fe(II)–citrate, Fe(II)–EDTA, Fe(II)–PPHA (Pahokee peat humic acid), or Fe(II)–SRFA (Suwannee river fulvic acid). In parallel, we also performed one cell suspension experiment with only non-OM-bound, free Fe(II). Oxidation of OM-complexed and free Fe(II) was compared by following concentrations of Fe(II) over time.

Bacterial Strain and Precultivation. The phototrophic Fe(II)-oxidizing bacterium *R. palustris* TIE-1 isolated from a marsh sediment⁹ is routinely cultivated in the authors' lab with 10 mM FeCl₂ in a basal medium.³⁰ To avoid transfer of Fe(III) minerals from the preculture, strain TIE-1 was grown and transferred three times in the basal medium without Fe(II) with H₂/CO₂ (80:20) as electron donor in the headspace before starting the incubation experiments with the different Fe(II) compounds.

Medium and Chemicals. The effects of four different ligands on Fe(II) oxidation rates were determined and compared to the rate and extent of oxidation of free non-OM-complexed Fe(II). The ligands tested were citrate, EDTA, PPHA, and SRFA. Experiments were conducted in anoxic PIPES-buffered media (pH 7) (prepared as in Peng et al.²⁹) to which 0.1 mM FeCl₂ and one of the chosen ligands were added. The concentration of ligand added varied between experiments to ensure complete complexation of the Fe(II). These concentrations were 0.2 mM, 0.12 mM, 0.2 mg/ml, and 0.2 mg/mL for citrate, EDTA, PPHA, and SRFA, respectively. Under these conditions, more than 99% of the Fe(II) was present as Fe(II)–OM complexes in each of the four individual Fe(II)–OM treatments according to geochemical modeling using PHREEQC coupled with a previously published humic ion-binding model (Model VI).^{51–53} This model takes the change of complexation capacity with concentration of OM into consideration and assumes that the complexation of Fe(II) by OM occurs through eight discrete sites. Five milliliters of anoxic medium was dispensed into 15 mL glass Hungate tubes³⁴ with airtight butyl-stoppers

and amended with 1 mM NaHCO₃ and 0.5% CO₂/99.5% N₂ in the headspace.

Setup of Experiments. Rates and extent of microbial oxidation of Fe(II)–OM complexes were determined in cell suspension experiments. In such experiments, no vitamins or trace metals are included in the medium so the cells are not expected to grow. For these experiments, the bacteria were cultured to the late exponential phase, harvested by centrifugation (7000 g, 20 min, 25 °C), washed twice, and resuspended in 20 mM anoxic PIPES buffer containing 20 mM NaCl in an anoxic glovebox (100% N₂). D/L staining (Thermo Fisher Scientific) showed that almost all the cells were alive after the washing steps (data not shown). An aliquot of the cell suspension (final cell number ca. 3.6 × 10⁷ cells/mL) was added to the medium containing either Fe(II)–citrate, Fe(II)–EDTA, Fe(II)–PPHA, or Fe(II)–SRFA complexes (four individual setups, no mixtures of complexes) in an anoxic glovebox. The tubes with the cell suspensions were incubated at 20 °C horizontally under a 40 W incandescent light bulb with a light intensity of ca. 550 lx; the thickness of the water layer in the tubes was ca. 5 mm.

Sample Analysis. Samples were taken using syringes in an anoxic glovebox (100% N₂) every 1–2 h. Fe(II) concentrations were determined anoxically using the ferrozine assay³⁵ modified as in Peng et al.²⁹ In brief, samples with non-OM-bound, free Fe(II), Fe(II)–citrate, and Fe(II)–EDTA complexes were first diluted with anoxic 1 M HCl to accelerate the formation of the Fe(II)–ferrozine complex, the last step of the ferrozine assay. Samples with Fe(II)–PPHA and Fe(II)–SRFA complexes were immediately mixed with ferrozine solution without 1 M HCl to avoid precipitation of HA and to avoid potential redox reactions of Fe with PPHA and SRFA during acidification. Total Fe concentrations were quantified by reduction of Fe(III) to Fe(II) by hydroxylamine hydrochloride 10% (w/v) in 1 M HCl.

The microbial oxidation products of free Fe(II) and Fe(II)–OM complexes were size-fractionated into dissolved (3 kDa MWCO; ca. 3 nm), colloidal (3 kDa to 0.2 μm), and particulate (>0.2 μm) fractions, and the concentrations of Fe(II) and Fe(III) within each fraction were determined. The fractionation was done anoxically in an anoxic chamber using Amicon Ultra-0.5 3 kDa ultrafiltration membranes (Millipore) and 0.2 μm PES filters (VMS). Cells were stained using BacLight Green (Thermo Fisher Scientific), and cell numbers were quantified by an Attune Nxt flow cytometer (Thermo

Fisher Scientific) equipped with a 488 nm laser as an excitation source. Cells were distinguished from noise or debris based on their properties in the side scatter and BL1 channel (with emission filter 530/30 nm).

Maximum rates of Fe(II) oxidation for the individual setups were calculated from the steepest slope between two subsequent data points of Fe(II) concentrations. All incubation and measurements were conducted in at least duplicates.

RESULTS AND DISCUSSION

Kinetics of Photoautotrophic Fe(II) Oxidation. To determine how Fe(II)–OM complexation influences the rates and extent of photoautotrophic Fe(II) oxidation, we performed four separate cell suspension experiments with the photoautotrophic Fe(II)-oxidizer *R. palustris* TIE-1 with either Fe(II)–citrate, Fe(II)–EDTA, Fe(II)–PPHA, or Fe(II)–SRFA complexes in parallel to a control setup with only non-OM-bound, free Fe(II), and followed concentrations of Fe(II) over time. We observed that the oxidation of Fe(II) by strain TIE-1 was faster when Fe(II) was present as Fe(II)–OM complexes compared to non-OM-bound, free Fe(II), although the extent of this stimulating effect varied for the different Fe(II)–OM complexes (Figure 1, Table 1). Fe(II)–

Table 1. Maximum Oxidation Rates of Free Fe(II) Compared to the Four Individual Fe(II)–OM Complexes by the Photoautotrophic Fe(II)-Oxidizer Strain TIE-1

form of Fe(II)	maximum oxidation rate	
	total ($\mu\text{M}/\text{h}$)	per cell pM/h/cell
Fe(II)–EDTA	126.7 ± 4.4	3.5
Fe(II)–citrate	100.7 ± 0.02	2.8
Fe(II)–SRFA	45.9 ± 1.5	1.3
Fe(II)–PPHA	20.7 ± 1.3	0.58
free Fe(II)	6.1 ± 1.3	0.17

EDTA complexes showed the fastest Fe(II) oxidation rates ($126.7 \pm 4.4 \mu\text{M}/\text{h}$) followed by Fe(II)–citrate ($100.7 \pm 0.02 \mu\text{M}/\text{h}$), Fe(II)–SRFA ($45.9 \pm 1.5 \mu\text{M}/\text{h}$), and Fe(II)–PPHA ($20.7 \pm 1.3 \mu\text{M}/\text{h}$), while the oxidation rate of free Fe(II) was only $6.1 \pm 1.3 \mu\text{M}/\text{h}$ (the \pm values indicate the range of rates calculated from duplicate experiments). The oxidation rates of Fe(II)–EDTA, Fe(II)–citrate, Fe(II)–PPHA, and Fe(II)–SRFA complexes were calculated to be 20.6-, 16.3-, 3.4-, and 7.5-fold faster, respectively, than that for free Fe(II). No Fe(II) was oxidized in abiotic controls without cells (Figure S1).

At pH 7 and 25 °C, the calculated redox potentials of Fe(II)–citrate and Fe(II)–EDTA complexes are more negative than the redox potential of aqueous Fe(II).^{36,37} Hence, the oxidation of Fe(II)–OM is thermodynamically more favorable than the oxidation of free Fe(II). This promotion of Fe(II) oxidation rates by OM may also explain what has been observed in some biotechnological studies, where systems containing Fe–OM complexes, e.g. Fe-citrate³⁸ and Fe-hexacyanoferrate,³⁹ showed a higher electron uptake by the photoautotrophic Fe(II)-oxidizer strain TIE-1 than from the electrodes.

In strain TIE-1, a decaheme c-type cytochrome, PioA, is thought to be the Fe(II)-oxidase; however, so far, the reaction rates for different Fe(II)–OM complexes with PioA have not been determined. In other cases with comparable microbial enzymatic Fe redox systems as in this study, it has been shown that different Fe(II)–OM complexes have different reaction

kinetics with bacterial c-type cytochromes, for example with MtoA of the microaerophilic Fe(II)-oxidizing bacterium *Sideroxydans lithotrophicus* ES-1,⁴⁰ MtrC and OmcA of Fe(III)-reducing bacterium *Shewanella oneidensis* MR-1,⁴¹ and an equine c-type cytochrome.⁴² It is currently not fully understood why these c-type cytochromes show different reaction kinetics with different forms of Fe(II). One plausible explanation could be a lower chemical activation energy for the oxidation of Fe(II)–OM complexes, which is related to both the reorganization energy and Gibbs free energy when Fe(II) is complexed by OM.⁴¹ Another possible explanation for the higher Fe(II) oxidation rates could be a better accessibility of the cytochrome to the Fe(II)–OM than to the free Fe(II). The surface of the cytochrome is known to be unevenly charged,^{43,44} and Fe(II)–OM complexation is expected to change the overall charge of the Fe(II) from positive to neutral or even negative,⁴⁵ potentially allowing a better interaction of the cytochrome with the Fe(II) species. Preferred oxidation of Fe(II)–OM compared to free Fe(II) may also provide a physiological benefit as the product of Fe(II)–OM oxidation could be water soluble or colloidal Fe(III)–OM complexes, while the oxidation of nonorganically bound Fe(II) would produce solid Fe(III) mineral particles that could be harmful to the cells due to encrustation. Preferential oxidation of Fe(II)–OM could thus negate the need to synthesize Fe(III)-binding ligands or adopt other energy-consuming mechanisms to avoid encrustation (such as establishment of low pH microenvironments).^{46–48}

Extent of Fe(II) Oxidation. Although we found that the Fe(II) oxidation rate was promoted by Fe(II)–OM complexation, there was still a significant portion of Fe(II) left at the end of the incubation (Figure 1). To better understand how OM complexation influences the products of photoautotrophic Fe(II) oxidation, we analyzed the particle/aggregate size of the products of oxidation of free Fe(II), Fe(II)–citrate, Fe(II)–PPHA, and Fe(II)–SRFA complexes (Figure 2). We chose to determine the size of the present Fe(II) and Fe(III) species

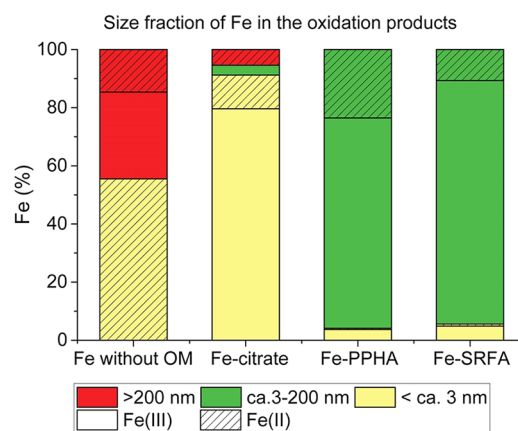


Figure 2. Size fractions of Fe in the oxidation products of free Fe(II) (Fe without OM), Fe(II)–citrate, Fe(II)–PPHA, and Fe(II)–SRFA at steady-state conditions after ca. 8.6 h of incubation (the last data point in Figure 1 when oxidation of free Fe(II) was not complete yet). The y-axis shows the percentages of Fe(II) and Fe(III) in a certain size fraction relative to the total concentration of Fe. Different size fractions are labeled with different colors; Fe(II) and Fe(III) are labeled with and without hatched patterns, respectively. The results are reported as an average calculated from two independent parallels and triplicate measurements.

after 8.6 h when Fe(II) concentrations were stable to minimize the potential effect of abiotic self-reorganization and recrystallization of Fe after the microbial oxidation of Fe(II)–OM complexes. For Fe–EDTA we determined only the size for Fe(II)–EDTA complexes, as the strong binding between Fe(III) and EDTA (stability constant $\log K = 16$)⁴⁹ seemed to interfere with the reduction of Fe(III) by hydroxylamine hydrochloride during the quantification of the total Fe (data not shown).

We found that Fe–OM complexation significantly changed the size fraction of the Fe oxidation products. Without OM complexation, after 8.6 h the oxidation of free Fe(II) was not complete due to the relatively slow Fe(II) oxidation rate, and all Fe(III) produced (ca. 30% of the total Fe) was in the particulate fraction (>200 nm). Interestingly, there was also approximately 15% Fe(II) in this particulate fraction, resulting in a ratio of Fe(II):Fe(III) of 1:2, probably in the form of Fe(II)–Fe(III)-phases such as magnetite (Fe₃O₄), green rust, or simply Fe(III) oxyhydroxides with associated Fe(II). This agrees with previous reports of Fe(II) being oxidized by strain TIE-1 resulting in the formation of Fe(III) oxyhydroxides and potentially magnetite.⁹ However, in the presence of OM, the size of the Fe(III) species produced was much smaller. Most of the Fe(III) was dissolved (ca. < 3 nm) in the oxidation products of Fe(II)–citrate or was present as colloids (between ca. 3–200 nm) in the oxidation products of Fe(II)–PPHA and Fe(II)–SRFA. The Fe(II) remaining at the end of the incubation with Fe(II)–citrate was in the particulate and dissolved fractions (ca. 5.6 and 11.6%, respectively) (Figure 2). In the experiments with Fe(II)–EDTA, the remaining Fe(II) was only in the dissolved fraction (data not shown), whereas the Fe(II) remaining at the end of the incubation with Fe(II)–PPHA and Fe(II)–SRFA was nearly all in the colloid fraction, which accounted for ca. 23.5 and 10.7% of the total Fe, respectively.

The size fractionation indicated that Fe(II)–OM complexation influences microbial photoautotrophic Fe(II) oxidation in several ways. First, the presence of colloidal Fe(II) remaining in the samples with PPHA and SRFA suggested that aggregation of Fe–PPHA and Fe–SRFA complexes as colloids may protect Fe(II) from microbial Fe(II) oxidation. This is probably due to a lack of accessibility of the c-type cytochromes to Fe(II) that is present in the inner part (core) of the Fe–OM colloids (the 3–200 nm fraction), as the maximum distance for electron transfer is very short, for example 2 nm.⁵⁰ Second, other possible factors such as the simultaneously occurring photoreduction of Fe(III)–citrate to Fe(II)⁵¹ and the change of redox potentials of Fe(II)/Fe(III) compared to free Fe(II) systems may also influence the remaining Fe(II) content.^{36,37} When the Fe(II)–OM and Fe(III)–OM complexes are not in the colloidal form but are completely dissolved, as it is the case for Fe(II)–/Fe(III)–citrate (Figure 2), these effects could be even more important than the size of the Fe(II) species present.

Environmental Implications. This study showed that Fe(II) complexation by OM significantly promoted microbial phototrophic Fe(II) oxidation. The higher oxidation rates observed for Fe(II)–OM complexes and the high abundance of such complexes in photic environments suggests that microbial Fe(II) oxidation in photic anoxic environments could be much more important than previously thought because most previous studies focused only on oxidation of nonorganically bound free Fe(II).^{9,52–54} Because photo-

autotrophic Fe(II) oxidation provides electrons during photosynthesis for CO₂ fixation,^{10,55,56} the Fe(II) oxidation stimulated by OM complexation may also promote the fixation of CO₂ and thus decrease CO₂ emission in Fe- and OM-rich environmental habitats, including surface layers of rice paddy soils and peatlands. On the other hand, our results have also revealed that part of the colloidal Fe(II)–OM was resistant to microbial photoautotrophic Fe(II) oxidation (Figure 2). This fraction of Fe(II) could be a sink for Fe(II) in the environment, as shown to be the case in the presence of a high C:Fe ratio,⁵⁷ where protection against abiotic oxidation by oxygen,²³ a decrease in the bioavailability of Fe,⁵⁸ and less oxidation by nitrate-dependent Fe(II)-oxidizing bacteria was observed.²⁹ Overall, this study indicates a close relationship between OM and Fe in the environment and shows that OM influences iron cycling not only by providing e-donors for microbial Fe(III) reduction^{59–62} but also by Fe-complexation which can strongly influence microbial phototrophic Fe(II) oxidation.

■ ASSOCIATED CONTENT

📄 Supporting Information

The Supporting Information is available free of charge on the ACS Publications website at DOI: 10.1021/acsearthspacechem.9b00024.

Figures S1 (abiotic controls of experiments) and S2 (oxidation of different complexes) (PDF)

■ AUTHOR INFORMATION

Corresponding Author

*Phone: +49-7071-2974992; Fax: +49-7071-29-295059; E-mail: andreas.kappler@uni-tuebingen.de.

ORCID

Chao Peng: 0000-0003-3433-4319

Thomas Borch: 0000-0002-4251-1613

Andreas Kappler: 0000-0002-3558-9500

Notes

The authors declare no competing financial interest.

■ ACKNOWLEDGMENTS

This work was supported by the Deutsche Forschungsgemeinschaft (DFG) grant KA 1736/36-1. We thank our technicians E. Röhm and L. Grimm for support in the lab.

■ REFERENCES

- (1) Lalonde, K.; Mucci, A.; Ouellet, A.; Gelinas, Y. Preservation of organic matter in sediments promoted by iron. *Nature* **2012**, *483* (7388), 198–200.
- (2) Hohmann, C.; Winkler, E.; Morin, G.; Kappler, A. Anaerobic Fe(II)-oxidizing bacteria show As resistance and immobilize As during Fe(III) mineral precipitation. *Environ. Sci. Technol.* **2010**, *44* (1), 94–101.
- (3) Zhu, Y.-G.; Xue, X.-M.; Kappler, A.; Rosen, B. P.; Meharg, A. A. Linking genes to microbial biogeochemical cycling: lessons from arsenic. *Environ. Sci. Technol.* **2017**, *51* (13), 7326–7339.
- (4) Muehe, E. M.; Adaktylou, I. J.; Obst, M.; Zeitvogel, F.; Behrens, S.; Planer-Friedrich, B.; Kraemer, U.; Kappler, A. Organic carbon and reducing conditions lead to cadmium immobilization by secondary Fe mineral formation in a pH-neutral soil. *Environ. Sci. Technol.* **2013**, *47* (23), 13430–13439.
- (5) Wang, H.; Yao, H.; Sun, P.; Li, D.; Huang, C.-H. Transformation of tetracycline antibiotics and Fe(II) and Fe(III) species induced by their complexation. *Environ. Sci. Technol.* **2016**, *50* (1), 145–153.

- (6) Melton, E. D.; Swanner, E. D.; Behrens, S.; Schmidt, C.; Kappler, A. The interplay of microbially mediated and abiotic reactions in the biogeochemical Fe cycle. *Nat. Rev. Microbiol.* **2014**, *12* (12), 797–808.
- (7) Bryce, C.; Blackwell, N.; Schmidt, C.; Otte, J.; Huang, Y.-M.; Kleindienst, S.; Tomaszewski, E.; Schad, M.; Warter, V.; Peng, C.; Byrne, J.; Kappler, A. Microbial anaerobic Fe(II) oxidation - ecology, mechanisms and environmental implications. *Environ. Microbiol.* **2018**, *20* (10), 3462–3483.
- (8) Madigan, M. T.; Clark, D. P.; Stahl, D.; Martinko, J. M. *Brock Biology of Microorganisms*, 13th ed.; Benjamin Cummings: 2010.
- (9) Jiao, Y.; Kappler, A.; Croal, L. R.; Newman, D. K. Isolation and characterization of a genetically tractable photoautotrophic Fe(II)-oxidizing bacterium, *Rhodospseudomonas palustris* strain TIE-1. *Appl. Environ. Microb.* **2005**, *71* (8), 4487–4496.
- (10) Jiao, Y.; Newman, D. K. The pio operon is essential for phototrophic Fe(II) oxidation in *Rhodospseudomonas palustris* TIE-1. *J. Bacteriol.* **2007**, *189* (5), 1765–1773.
- (11) Shi, L.; Dong, H.; Reguera, G.; Beyenal, H.; Lu, A.; Liu, J.; Yu, H.-Q.; Fredrickson, J. K. Extracellular electron transfer mechanisms between microorganisms and minerals. *Nat. Rev. Microbiol.* **2016**, *14*, 651.
- (12) Byrne, J. M.; Klueglein, N.; Pearce, C.; Rosso, K. M.; Appel, E.; Kappler, A. Redox cycling of Fe(II) and Fe(III) in magnetite by Fe-metabolizing bacteria. *Science* **2015**, *347* (6229), 1473–1476.
- (13) Bose, A.; Gardel, E. J.; Vidoudez, C.; Parra, E. A.; Girguis, P. R. Electron uptake by iron-oxidizing phototrophic bacteria. *Nat. Commun.* **2014**, *5*, 3391.
- (14) Hopwood, M. J.; Statham, P. J.; Skrabal, S. A.; Willey, J. D. Dissolved iron(II) ligands in river and estuarine water. *Mar. Chem.* **2015**, *173*, 173–182.
- (15) Luther, G. W.; Shellenbarger, P. A.; Brendel, P. J. Dissolved organic Fe(III) and Fe(II) complexes in salt marsh porewaters. *Geochim. Cosmochim. Acta* **1996**, *60* (6), 951–960.
- (16) Sundman, A.; Karlsson, T.; Persson, P. An experimental protocol for structural characterization of Fe in dilute natural waters. *Environ. Sci. Technol.* **2013**, *47* (15), 8557–8564.
- (17) von der Heyden, B. P.; Hauser, E. J.; Mishra, B.; Martinez, G. A.; Bowie, A. R.; Tylliszczak, T.; Mshali, T. N.; Roychoudhury, A. N.; Myneni, S. C. B. Ubiquitous presence of Fe(II) in aquatic colloids and its association with organic carbon. *Environ. Sci. Technol. Lett.* **2014**, *1* (10), 387–392.
- (18) Sundman, A.; Karlsson, T.; Laudon, H.; Persson, P. XAS study of iron speciation in soils and waters from a boreal catchment. *Chem. Geol.* **2014**, *364*, 93–102.
- (19) Bhattacharyya, A.; Schmidt, M. P.; Stavitski, E.; Martínez, C. E. Iron speciation in peats: chemical and spectroscopic evidence for the co-occurrence of ferric and ferrous iron in organic complexes and mineral precipitates. *Org. Geochem.* **2018**, *115*, 124–137.
- (20) Kleja, D. B.; van Schaik, J. W. J.; Persson, I.; Gustafsson, J. P. Characterization of iron in floating surface films of some natural waters using EXAFS. *Chem. Geol.* **2012**, *326–327*, 19–26.
- (21) Yu, C.; Virtasalo, J. J.; Karlsson, T.; Peltola, P.; Österholm, P.; Burton, E. D.; Arppe, L.; Hogmalm, J. K.; Ojala, A. E. K.; Åström, M. E. Iron behavior in a northern estuary: large pools of non-sulfidized Fe(II) associated with organic matter. *Chem. Geol.* **2015**, *413*, 73–85.
- (22) Barbeau, K. Photochemistry of organic iron(III) complexing ligands in oceanic systems. *Photochem. Photobiol.* **2006**, *82* (6), 1505–1516.
- (23) Daugherty, E. E.; Gilbert, B.; Nico, P. S.; Borch, T. Complexation and redox buffering of iron(II) by dissolved organic matter. *Environ. Sci. Technol.* **2017**, *51* (19), 11096–11104.
- (24) Lee, Y. P.; Fujii, M.; Kikuchi, T.; Terao, K.; Yoshimura, C. Variation of iron redox kinetics and its relation with molecular composition of standard humic substances at circumneutral pH. *PLoS One* **2017**, *12* (4), No. e0176484.
- (25) Rose, A. L.; Waite, T. D. Effect of dissolved natural organic matter on the kinetics of ferrous iron oxygenation in seawater. *Environ. Sci. Technol.* **2003**, *37* (21), 4877–4886.
- (26) Chen, C.; Thompson, A. Ferrous iron oxidation under varying pO₂ levels: the effect of Fe(III)/Al(III) oxide minerals and organic matter. *Environ. Sci. Technol.* **2018**, *52* (2), 597–606.
- (27) Kopf, S. H.; Henny, C.; Newman, D. K. Ligand-enhanced abiotic iron oxidation and the effects of chemical versus biological iron cycling in anoxic environments. *Environ. Sci. Technol.* **2013**, *47* (6), 2602–2611.
- (28) Neubauer, E.; Köhler, S. J.; von der Kammer, F.; Laudon, H.; Hofmann, T. Effect of pH and stream order on iron and arsenic speciation in boreal catchments. *Environ. Sci. Technol.* **2013**, *47* (13), 7120–7128.
- (29) Peng, C.; Sundman, A.; Bryce, C.; Catrouillet, C.; Borch, T.; Kappler, A. Oxidation of Fe(II)–organic matter complexes in the presence of the mixotrophic nitrate-reducing Fe(II)-oxidizing bacterium *Acidovorax* sp. BoFeN1. *Environ. Sci. Technol.* **2018**, *52* (10), 5753–5763.
- (30) Melton, E. D.; Schmidt, C.; Kappler, A. Microbial iron(II) oxidation in littoral freshwater lake sediment: the potential for competition between phototrophic vs. nitrate-reducing iron(II)-oxidizers. *Front. Microbiol.* **2012**, *3*, 197.
- (31) Catrouillet, C.; Davranche, M.; Dia, A.; Bouhnik-Le Coz, M.; Marsac, R.; Pourret, O.; Gruau, G. Geochemical modeling of Fe(II) binding to humic and fulvic acids. *Chem. Geol.* **2014**, *372*, 109–118.
- (32) Marsac, R.; Davranche, M.; Gruau, G.; Bouhnik-Le Coz, M.; Dia, A. An improved description of the interactions between rare earth elements and humic acids by modeling: PHREEQC-Model VI coupling. *Geochim. Cosmochim. Acta* **2011**, *75* (19), 5625–5637.
- (33) Tipping, E. Humic ion-binding model VI: an improved description of the interactions of protons and metal ions with humic substances. *Aquat. Geochem.* **1998**, *4* (1), 3–47.
- (34) Macy, J. M.; Snellen, J. E.; Hungate, R. E. Use of syringe methods for anaerobiosis. *Am. J. Clin. Nutr.* **1972**, *25* (12), 1318–1323.
- (35) Stookey, L. L. Ferrozine—a new spectrophotometric reagent for iron. *Anal. Chem.* **1970**, *42* (7), 779–781.
- (36) Buerge, I. J.; Hug, S. J. Influence of Mineral Surfaces on Chromium(VI) Reduction by Iron(II). *Environ. Sci. Technol.* **1999**, *33* (23), 4285–4291.
- (37) Naka, D.; Kim, D.; Strathmann, T. J. Abiotic Reduction of Nitroaromatic Compounds by Aqueous Iron(II)–Catechol Complexes. *Environ. Sci. Technol.* **2006**, *40* (9), 3006–3012.
- (38) Doud, D. F. R.; Angenent, L. T. Toward electrosynthesis with uncoupled extracellular electron uptake and metabolic growth: enhancing current uptake with *Rhodospseudomonas palustris*. *Environ. Sci. Technol. Lett.* **2014**, *1* (9), 351–355.
- (39) Rengasamy, K.; Ranaivoarisoa, T.; Singh, R.; Bose, A. An insoluble iron complex coated cathode enhances direct electron uptake by *Rhodospseudomonas palustris* TIE-1. *Bioelectrochemistry* **2018**, *122*, 164–173.
- (40) Liu, J.; Wang, Z.; Belchik, S. M.; Edwards, M. J.; Liu, C.; Kennedy, D. W.; Merkley, E. D.; Lipton, M. S.; Butt, J. N.; Richardson, D. J.; Zachara, J. M.; Fredrickson, J. K.; Rosso, K. M.; Shi, L. Identification and characterization of MtoA: a decaheme c-type cytochrome of the neutrophilic Fe(II)-oxidizing bacterium *Sideroxydans lithotrophicus* ES-1. *Front. Microbiol.* **2012**, *3*, 37.
- (41) Wang, Z.; Liu, C.; Wang, X.; Marshall, M. J.; Zachara, J. M.; Rosso, K. M.; Dupuis, M.; Fredrickson, J. K.; Heald, S.; Shi, L. Kinetics of reduction of Fe(III) complexes by outer membrane cytochromes MtrC and OmcA of *Shewanella oneidensis* MR-1. *Appl. Environ. Microb.* **2008**, *74* (21), 6746–6755.
- (42) Wang, Y.; Li, X.; Liu, T.; Li, F. The reaction between c-type cytochromes and Fe(II): ligand effects and mechanisms. *Goldschmidt Abstr.* **2017**, 4177.
- (43) Pereira, L.; Saraiva, I. H.; Oliveira, A. S. F.; Soares, C. M.; Louro, R. O.; Frazão, C. Molecular structure of FoxE, the putative iron oxidase of *Rhodobacter ferrooxidans* SW2. *Biochim. Biophys. Acta, Bioenerg.* **2017**, *1858* (10), 847–853.
- (44) Leys, D.; Meyer, T. E.; Tsapin, A. S.; Neilson, K. H.; Cusanovich, M. A.; Van Beeumen, J. J. Crystal structures at atomic

resolution reveal the novel concept of “electron-harvesting” as a role for the small tetraheme cytochrome *c*. *J. Biol. Chem.* **2002**, *277* (38), 35703–35711.

(45) Grinberg, A. A. *An Introduction to the Chemistry of Complex Compounds*; Elsevier: 2013.

(46) Chan, C. S.; De Stasio, G.; Welch, S. A.; Girasole, M.; Frazer, B. H.; Nesterova, M. V.; Fakra, S.; Banfield, J. F. Microbial polysaccharides template assembly of nanocrystal fibers. *Science* **2004**, *303* (5664), 1656–1658.

(47) Miot, J.; Benzerara, K.; Obst, M.; Kappler, A.; Hegler, F.; Schädler, S.; Bouchez, C.; Guyot, F.; Morin, G. Extracellular iron biomineralization by photoautotrophic iron-oxidizing bacteria. *Appl. Environ. Microb* **2009**, *75* (17), 5586–5591.

(48) Hegler, F.; Schmidt, C.; Schwarz, H.; Kappler, A. Does a low-pH microenvironment around phototrophic Fe(II)-oxidizing bacteria prevent cell encrustation by Fe(III) minerals? *FEMS Microbiol. Ecol.* **2010**, *74* (3), 592–600.

(49) Martell, A.; Smith, R.; Motekaitis, R. NIST critical stability constants of metal complexes database. US Department of Commerce: Gaithersburg, 1993.

(50) Gray, H. B.; Winkler, J. R. Electron flow through proteins. *Chem. Phys. Lett.* **2009**, *483* (1), 1–9.

(51) Frahn, J. The photochemical decomposition of the citrate-ferric iron complex: A study of the reaction products by paper ionoporesis. *Aust. J. Chem.* **1958**, *11* (4), 399–405.

(52) Laufer, K.; Byrne, J. M.; Glombitza, C.; Schmidt, C.; Jørgensen, B. B.; Kappler, A. Anaerobic microbial Fe(II) oxidation and Fe(III) reduction in coastal marine sediments controlled by organic carbon content. *Environ. Microbiol.* **2016**, *18* (9), 3159–3174.

(53) Hegler, F.; Posth, N. R.; Jiang, J.; Kappler, A. Physiology of phototrophic iron(II)-oxidizing bacteria: implications for modern and ancient environments. *FEMS Microbiol. Ecol.* **2008**, *66* (2), 250–260.

(54) Ehrenreich, A.; Widdel, F. Anaerobic oxidation of ferrous iron by purple bacteria, a new type of phototrophic metabolism. *Appl. Environ. Microb* **1994**, *60* (12), 4517–4526.

(55) Bird, L. J.; Bonnefoy, V.; Newman, D. K. Bioenergetic challenges of microbial iron metabolisms. *Trends Microbiol.* **2011**, *19* (7), 330–340.

(56) Widdel, F.; Schnell, S.; Heising, S.; Ehrenreich, A.; Assmus, B.; Schink, B. Ferrous iron oxidation by anoxygenic phototrophic bacteria. *Nature* **1993**, *362* (6423), 834–836.

(57) Liao, P.; Li, W.; Jiang, Y.; Wu, J.; Yuan, S.; Fortner, J. D.; Giammar, D. E. Formation, aggregation, and deposition dynamics of NOM-iron colloids at anoxic–oxic interfaces. *Environ. Sci. Technol.* **2017**, *51* (21), 12235–12245.

(58) Oleinikova, O. V.; Shirokova, L. S.; Gérard, E.; Drozdova, O. Y.; Lapitskiy, S. A.; Bychkov, A. Y.; Pokrovsky, O. S. Transformation of organo-ferric peat colloids by a heterotrophic bacterium. *Geochim. Cosmochim. Acta* **2017**, *205*, 313–330.

(59) Roden, E. E.; Kappler, A.; Bauer, I.; Jiang, J.; Paul, A.; Stoesser, R.; Konishi, H.; Xu, H. Extracellular electron transfer through microbial reduction of solid-phase humic substances. *Nat. Geosci.* **2010**, *3*, 417.

(60) Amstatter, K.; Borch, T.; Kappler, A. Influence of humic acid imposed changes of ferrihydrite aggregation on microbial Fe(III) reduction. *Geochim. Cosmochim. Acta* **2012**, *85*, 326–341.

(61) Shimizu, M.; Zhou, J. H.; Schroder, C.; Obst, M.; Kappler, A.; Borch, T. Dissimilatory reduction and transformation of ferrihydrite-humic acid coprecipitates. *Environ. Sci. Technol.* **2013**, *47* (23), 13375–13384.

(62) Jiang, J.; Kappler, A. Kinetics of microbial and chemical reduction of humic substances: implications for electron shuttling. *Environ. Sci. Technol.* **2008**, *42* (10), 3563–3569.